IEEE Access
Multidisciplinary ⋮ Rapid Review ⋮ Open Access Journal

Received 27 December 2022, accepted 27 January 2023, date of publication 6 February 2023, date of current version 10 February 2023.

Digital Object Identifier 10.1109/ACCESS.2023.3242611

RESEARCH ARTICLE

Position Estimation of Radio Source Based on Fingerprinting With Physical Wireless Parameter Conversion Sensor Networks

MASAFUMI ODA[1], OSAMU TAKYU[1], (Member, IEEE), MAI OHTA[2], (Member, IEEE), TAKEO FUJII[3], (Member, IEEE), AND KOICHI ADACHI[3], (Senior Member, IEEE)

[1]Department of Electrical and Computer Engineering, Shinshu University, Nagano 380-8553, Japan
[2]Department of Electronics Engineering and Computer Science, Fukuoka University, Fukuoka 814-0180, Japan
[3]Advanced Wireless and Communication Research Center, The University of Electro-Communications, Chofu, Tokyo 182-8585, Japan

Corresponding author: Osamu Takyu (takyu@shinshu-u.ac.jp)

This work was supported in part by the Ministry of Internal Affairs and Communications Strategic Information and Communications Research and Development Promotion Programme (SCOPE) under Grant JP205004001, and in part by the Japan Society for the Promotion of Science (JSPS) Kaken under Grant JP21H01322.

ABSTRACT Establishing a highly accurate positioning of radio sources for radio wave monitoring and frequency spectrum sharing is attracting considerable attention. Because the positioning method generally requires specific processing of the position target, it is not applicable when the position target cannot perform any processing. The location fingerprinting method uses multiple sensors to observe the received signal strength indication (RSSI) emitted by a radio source and estimates the position from the radio wave propagation characteristics. This does not require a certain process for the target position. However, it takes time to gather RSSI from many sensors by wireless communication. In this study, we propose an RSSI gathering method using physical wireless parameter conversion sensor networks (PhyC-SN) for the high-speed positioning of radio sources. In the proposed method, each sensor selects the radio carrier frequency corresponding to its measured RSSI and transmits the signal. Projecting the RSSI distribution of each sensor onto the frequency distribution of the received signal enables the center to detect the RSSI of multiple sensors simultaneously. Furthermore, to improve the gathering accuracy, we established a sensor group method by considering the regional characteristics and access timing control based on each sensor group. Computer simulations and experimental evaluations show that the proposed method significantly reduces the data-gathering time compared with conventional packet communications and achieves a high positioning accuracy.

INDEX TERMS Location fingerprinting, PhyC-SN.

I. INTRODUCTION

Recently, many services using location information have been provided, and various studies have been conducted to advance the location estimation technology [1]. The most famous positioning scheme is the global positioning system (GPS) [2]. However, GPS cannot be used in indoor environments because it requires the reception of signals emitted from multiple satellites. Additionally, it is necessary to attach a GPS receiver to the target position. It is difficult to attach a receiving device for positioning to a phenomenon that spontaneously generates a positioning target, such as a heat source [3] or an earthquake source [4]. Moreover, it is impossible to attach a receiving device for positioning to an illegal radio source in a radio monitoring system [5] and the primary access wireless system for frequency spectrum sharing [6].

Various positioning methods that do not use reception processing for positioning the targets have been considered. Positioning methods using spatial ripple effects have been studied when the positioning target is the wave source. Specifically, the centroid method based on the received signal strength indication (RSSI) of the radio source [6], a method

The associate editor coordinating the review of this manuscript and approving it for publication was Hongwei Du.

using the angle of arrival and arrival time of the sound source [7], and the location fingerprinting method [8], which utilizes the spatial peculiarity of ripple effects such as the heat source for enlarging the temperature and the radio source for enlarging the RSSI, have been proposed. In these methods, many sensors that measure characteristics such as the strength of the ripple effect are placed uniformly within the observation range in advance, and they inform the sensing data to the data center station via wireless sensor networks (WSN). To improve the positioning accuracy, sensors need to be set with fine spatial granularity; therefore, it is necessary to gather sensing data from a large number of sensors.

In the fifth-generation wireless communication standard (5G), massive machine-type communication (mMTC) supports a large amount of sensor information [9]. Its large running cost and complicated procedure are barriers to its introduction. The low-power wide area (LPWA) is attracting attention as a WSN operating in unlicensed frequency bands [10]. To deal with packet access from many sensors, orthogonal radio resource allocation with time and frequency division multiple access is required. Reference [11] proposed a method to gather sensor information at high speed by time-division multiple access, where the unit of time for a packet access is defined as a slot. Because an exclusive time slot should be assigned to each sensor for packet access, and the waiting time for packet collision avoidance is necessary, the time required for data gathering is long. Simultaneous access among multiple sensors by non-orthogonal multiple access (NOMA), which demodulates using the power difference of packets, is considered [12]. NOMA fails to demodulate packets owing to multipath fading, and thus, the steadying of data gathering is difficult. Positioning results can be used for evacuation during disasters, such as earthquakes [4], control applications [13], and protection of existing systems during frequency spectrum sharing [14]. It is necessary to gather sensor information in a short period of time, and it has been pointed out that the time taken to gather sensor information by a WSN is a large overhead [11]. To our best knowledge, the positioning scheme without requiring the receiving device attached to the positioning target as well as with the short time by completing the position estimation has not been considered, yet.

Physical wireless parameter conversion sensor networks (PhyC-SNs) have been proposed as a communication method that enables the simultaneous access of multiple sensors [15]. Each sensor transmits a carrier by switching the carrier frequency according to the sensing data. Although multiple sensors simultaneously access the data center by emitting the carrier, the intensity of the sensor data appears as a power distribution of the frequency spectrum of the received signals. Therefore, the sensor information of all sensors can be detected instantaneously by determining the existence of the signal from the power distribution. Therefore, using PhyC-SN to collect sensor data for positioning, the realization of positioning within a short time is expected, but it has not been clarified yet.

This study proposes a positioning method based on fingerprints [8] using the PhyC-SN for sensor data gathering from multiple sensors. Each sensor measured the RSSI when the positioning target was a radio source. Each sensor transmits a carrier whose center frequency is determined by the measured RSSI value. The proposed positioning method has two phases: a pre-observation phase and an estimation phase. In the pre-observation phase, the position of the target is known, and each sensor measures the RSSI. The RSSI is then sent to the data center by PhyC-SN. The center station analyzes the frequency spectrum of the received signal and then counts the number of carriers with power over a certain threshold in each frequency sub-band. The center station recognizes the number of informed RSSIs. The dataset is composed of the number of informed RSSIs and the position information of the positioning target. In the estimation phase, when the position of the position target is not determined, each sensor measures the RSSI and then informs the measured RSSI of the center station by the PhyC-SN. The center station counts the RSSIs in the same manner as in the pre-observation phase. The center station selects one dataset among the datasets measured by the pre-observation phase in terms of the minimum squared Euclidean distance criterion from the dataset measured by the estimation phase. The location information indicated in the selected dataset was considered as the estimated location of the positioning target.

In data gathering by PhyC-SN, the number of sensors is estimated from the magnitude of the power of the frequency component to deduce that multiple sensors select and transmit the same frequency component [16]. Its accuracy is significantly degraded owing to the power fluctuations caused by multipath fading. In this study, we establish an ''on-off identification'' with a single threshold to determine whether more than one sensor is transmitted. Consequently, the effect of the power fluctuation caused by multipath fading is limited. However, as the number of sensors becomes uncertain, the identification accuracy of the sensor information deteriorates. Because each sensor measures various RSSI, although the information on the number of sensors is lost due to the ''on-off identification,'' the tendency of the spatial distribution of RSSI is not completely lost, and it can be used as a location fingerprinting method.

Furthermore, we introduce time-division transmission, in which sensors are formed into multiple groups, and the particular access timing to the data center is assigned to each group. This can reduce the number of sensors that transmit simultaneously, the number of sensors that notify the same RSSI, and the number of sensors that become indefinite owing to the ''on-off identification''. Furthermore, by considering the regional characteristics in the design of the observation area, we can improve the accuracy of identifying the regional characteristics of the measured RSSI as well as the positioning accuracy.

The contributions of this study are as follows: 1. We established a positioning method using PhyC-SN as a data-gathering scheme for many sensors. It was shown that a significant reduction in the gathering time and equivalent positioning accuracy compared to the packet access was achieved. The effectiveness of this method was demonstrated through computer simulations and experimental evaluation.

2. To mitigate the effects of power fluctuations that occur at the time of aggregation in PhyC-SN, we establish an ''on-off identification'' method.

3. We established a sensor group construction method and a time division transmission method that are excellent in improving the identification accuracy of gathered information by '' on-off identification'' and measuring the regional characteristics of the observation area.

Authors in an international conference proposed the application of PhyC-SN location fingerprinting [17]. There is no discussion on countermeasures against the influence of deterioration in the identification accuracy of the number of sensors caused by power fluctuations during aggregation. Furthermore, Reference [18], who proposed a method of forming sensor groups, did not fully consider the effectiveness of group formation, and the policy of the formation method was unclear. In this study, we propose the ''on-off identification'' as a new method for recognizing the sensing data in PhyC-SN to maintain the robustness of the power fluctuations. Furthermore, we consider three types of sensor grouping methods and clarify the suitable sensor grouping for improving the location accuracy of the radio source. Computer simulation results have shown that the required data gathering time of the proposed scheme is shorter than 1/17 of the conventional packet access scheme with the same positioning accuracy

The remainder of this paper is organized as follows. Section II presents conventional studies related to this work. Section III explains the assumed positioning system based on WSN. Section IV presents the details of the proposed fingerprinting method based on PhyC-SN. Sections V and VI present the numerical results of the computer simulation and experimental evaluation, respectively. Section VII presents the conclusions of the study.

II. RELATED PAPERS

As a positioning method that uses a sensor network, the position estimation method is based on the center of gravity, which is referred to as the centroid method. This method estimates the position by adding the position information of each sensor and weighting the RSSI measured by it [19]. Referefence [20] proposed the improvement of the positioning accuracy of the centroid method. To achieve this, a gathering scheme based on packet communication from each sensor to the center station was proposed [11]. However, data gathering takes a long time, which causes a delay in the position estimation.

The time-of-arrival (ToA) positioning method was proposed to reduce the effects of fading in NLOS environments using high-gain antennas in sensor radios [21]. It is necessary to specify the time, and a specific method for time acquisition has not yet been considered. Reference [22] actively discussed positioning methods using sensor networks from the viewpoint of security.

Positioning methods that conform to the wireless communication standards have also been proposed. Positioning methods using the IEEE 802.11 standard (WiFi) have been proposed mainly for indoor positioning. Positioning is performed by constructing a database using the MAC address of the access point in the location fingerprinting method, which uses the RSSI of Wi-Fi. The database was used as pre-learning data, and a probabilistic model of the RSSI was applied to improve the positioning accuracy [23]. In IEEE 802.11mc, the Wi-Fi round-trip time was also proposed for positioning [24]. However, the processing delay directly impacted the degradation of the position accuracy.

Positioning methods using various wireless standards other than Wi-Fi have also been proposed. A multivariable fingerprint based on the observable received parameters in 5GNR was proposed [25]. The annealing and genetic algorithms for optimization are applied to the fingerprint based on the RSSI of Zigbee [26]. As a joint positioning method, a positioning method using 2.4 GHz and 5.8 GHz Wi-Fi RSSI and Deep Neural Network (DNN) is proposed, and the positioning accuracy is improved by combining the characteristics of radio wave propagation that differ depending on the frequency band [27]. However, all of them are premised on establishing communication with a measurement target and are difficult to apply to a positioning target without a communication function.

The construction method of the database for location fingerprinting was considered. A dedicated collector was used to measure the RSSI of Wi-Fi and automatically create a database for indoor fingerprinting [28]. An update of the database for fingerprinting assisted by IoT sensors was proposed [29]. Reference [30] proposed a uniform platform for the construction of a map and real time navigation, which is necessary for the entire process of the indoor positioning system based on fingerprinting. As the database for fingerprinting is constructed using the above schemes, methods for positioning within a short time are required.

Position fingerprinting based on the RSSI of Wi-Fi has been considered [31]. Its positioning accuracy can be improved by the combined use of other types of sensing data, such as accelerometers, gyroscopes, and geomagnetic sensors, and an adaptive quantum filter compensates for the non-line-of-sight error. A dead reckoning scheme with mobility of the positioning target and map information was considered [32], [33], [34]. It is still available even when the RSSI and geomagnetism are lost. Additionally, a method was proposed to improve the positioning accuracy using sensors from the inertial measurement unit along with positioning by RSSI fingerprints using machine learning recurrent neural networks and conditional generative adversarial networks [35]. However, the above positioning methods depend

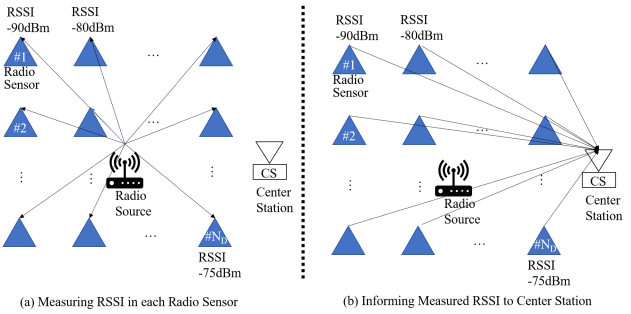

FIGURE 1. System overview of radio source positioning system based on radio sensors.

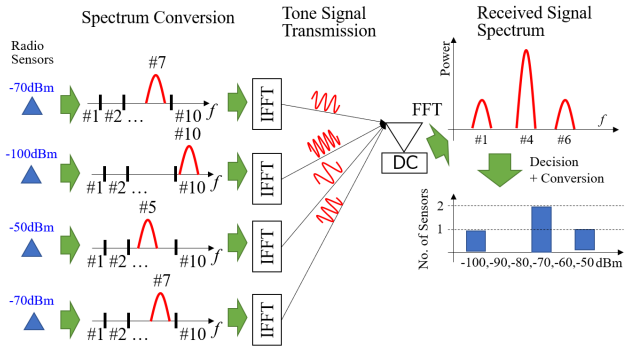

FIGURE 2. Communication method of PhyC-SN.

on the process of the positioning target; thus, they are unavailable without the assistance of the positioning target.

A scheme for improving the accuracy of indoor positioning is considered. In the position fingerprint, a probabilistic model of the RSSI is assumed to mitigate the fluctuations of the RSSI, and the positioning accuracy is improved by the k-nearest neighbor (k-NN) method [36]. A modified k-NN method for improving the position accuracy was proposed [37]. Position fingerprinting with the RSSI measured by large radio sensors is applied to a support vector machine (SVM) to improve the position accuracy [38]. A correction method using a Kalman filter for indoor positioning results was proposed [39]. A correction to the position estimation method of RSSI-based fingerprinting using a gradient descent algorithm was proposed [40]. However, in these schemes, the positioning target must measure the RSSI.

Many of the studies thus far require positioning processing, such as signal reception processing and RSSI measurement for the positioning target. Additionally, in the centroid method and the positional fingerprint method, a method is proposed in which a large number of sensors measure the RSSI, eliminating the need for reception processing and measurement by the observation target. However, gathering information from a large number of sensors in a short period of time requires an enormous amount of resources, and delays due to the consumption of frequency and time resources are a serious problem. A short-time positioning method, including a method for gathering sensor information, has not been sufficiently studied.

III. SYSTEM OVERVIEW

A. RADIO SENSOR NETWORKS

Figure 1 shows an overview of the radio source positioning system based on the WSN system assumed in this study. The radio sensors were placed uniformly within the area of interest. Each sensor has a sensing function to measure the RSSI and a wireless function to transfer the measured RSSI to the center station (CS). We assume that the RSSI is the sensor information. We also assume that the frequency band measured by the sensor function is different from that accessed by the wireless function.

TABLE 1. Mapping table between subcarrier number and RSSI.

Subcarrier Number	RSSI (dBm)
1	-10
2	-20
3	-30
4	-40
5	-50
6	-60
7	-70
8	-80
9	-90
10	-100

B. DATA GATHERING BY PhyC-SN

All the radio sensors report the detected RSSI to the CS via wireless communication. Therefore, we assumed a star-shaped network topology with access from multiple sensors to one CS. The CS broadcasts a control signal indicating a sensor information notification request for all sensors. The sensor receives control signals and transmits the detected sensor information to the CS. It is assumed that the access timing is corrected by the notification of the control signal and that the access timing error of each sensor is shorter than that of the CS, where the signal detection interval is determined by the frequency resolution of the fast Fourier transform (FFT). Consequently, the transmission signals of all the sensors were present in the signal detection interval.

PhyC-SN is used [15] as a communication method for transmitting the RSSI of each sensor to the CS. Figure 2 shows an image of the data-gathering flow by PhyC-SN. First, the detected RSSI were quantized at regular intervals. Consequently, the magnitude of the RSSI was converted to an integer value. PhyC-SN is premised on orthogonal frequency-division multiplexing (OFDM), divides the entire occupied band into narrow bands of fixed divisions, and transmits on subcarriers with the center frequency of the narrow band. At this point, a subcarrier number corresponding to the RSSI level was assigned. A table corresponding to the RSSI levels and subcarrier numbers is generated and stored in the transmitter and receiver, where the table is referred to as the conversion table. Table 1 shows the mapping table

used by figure 2. The radio sensor, which is the transmitter, selects a subcarrier number corresponding to the conversion table. Subsequently, a continuous sine wave is transmitted to the subcarrier of the selected subcarrier number, and the other subcarriers are not used but are assigned to nulls. The receiver detects the frequency component of the subcarrier based on the FFT after detecting the received signal for the detection time interval. When a subcarrier is transmitted at the transmitter, the frequency components of the subcarrier detected at the receiver exhibit high power. Therefore, the power of the frequency component of each subcarrier is compared with a predetermined threshold, and if the power is greater than or equal to the threshold, the transmitter transmits the signal. The receiver can recognize the transmitted RSSI level according to the conversion table. In the PhyC-SN, each sensor informs the measured RSSI to the CS by using the particular subcarrier corresponding to the measured RSSI.

Next, we consider a case in which a plurality of radio sensors transmits signals. In PhyC-SN, the transmitted signal does not have a sensor-specific ID; therefore, the receiver does not specify the radio sensor, which is the transmit information source of the detected RSSI. If a plurality of radio sensors detects the same RSSI level and transmits it with the same subcarrier, the signals of the plurality of subcarriers are combined and received. In this case, the average power of the frequency components detected by the receiver increases according to the number of sensors. Therefore, we used a multilevel threshold to identify the number of sensors that transmit the same subcarrier. However, the power of the combined signal fluctuates significantly because of the asynchronous combination of multiple subcarriers and multipath fading. Because the physical distance between each sensor and CS is different, the propagation loss is different for each sensor. To simplify the configuration of the sensors, the average received power was also different for each sensor when transmission power control was not applied. Consequently, the accuracy of identifying the number of subcarriers using the threshold values of multiple stages is significantly degraded.

C. POSITION FINGERPRINTING

The location fingerprinting method has two phases of processing: the pre-observation phase, and the position-estimation phase. The radio frequency fingerprint is considered as one of the supervising learnings. The pre-observation phase is considered as the training with the radio source with known position. The position-estimation phase is the actual location estimation of the radio source with unknown position.

In the pre-observation phase, the radio source to be positioned is equipped with a device capable of positioning (eg, a global positioning system (GPS), etc.). Therefore, in the pre-observation phase, the position of the radio source was used as teacher data. The radio sources were placed at various positions within the target area. Each radio sensor transmits the measured RSSI to the CS. In the following explanation of conventional position fingerprinting, we assume a packet access scheme for gathering data from the sensors. The RSSI was added to the payload, and the ID of the transmitting station was added to the header and transmitted to the CS. The CS gathers the ID and RSSI datasets from all sensors. Here, the dth radio sensor ($d \in 1, 2, \ldots, N_D$) at the lth source ($l \in 1, 2, \ldots, N_L$) measures the RSSI as p_d^l, where N_L and N_D are the total number of radio source positions and the total number of radio sensors placed in the pre-observation phase, respectively. Consequently, the RSSI distribution of the radio sensor at the lth radio source is given by

$$\boldsymbol{p}^l = [p_1^l, p_2^l, \ldots, p_{N_D}^l]. \tag{1}$$

This RSSI distribution is defined as the location fingerprint vector of the lth radio source.

Next, in the position-estimation phase, there is no device capable of positioning with respect to the radio source. The CS sends control signals to all the sensors to provide a position estimate of the radio source. Consequently, each sensor measures the RSSI and then sends it to the CS with the sensor ID by packet access. The CS receives the RSSIs from all sensors with the sensor ID. Subsequently, it constructs the following location fingerprint vector.

$$\boldsymbol{p}^* = [p_1^*, p_2^*, \ldots, p_{N_D}^*]. \tag{2}$$

From the position fingerprint vectors of the pre-observation phase, the position of the source in advance $l^\star$ is specified by the minimum squared Euclidean distance criterion between the position fingerprint vectors in the pre-observation and position estimation phases. Thus, the following formula was obtained:

$$l^\star = \arg\min_{\forall l} (\boldsymbol{p}^* - \boldsymbol{p}^l)(\boldsymbol{p}^* - \boldsymbol{p}^l)^T, \tag{3}$$

where $()^T$ denotes the vector transposition. The position of the radio source specified in the pre-observation phase in $l^\star$ is considered as the position of the radio source to be estimated.

In the position fingerprint method, the position estimation error is the difference in the distance between the actual position of the radio source and the position of the nearby radio source estimated in the pre-observation phase. This can be suppressed if the spatial resolution of the radio sources in the pre-observation phase is finer. It is difficult that the radio source in the position-estimation phase is perfectly matched to the radio sources in the pre-observation phase. This reason is as follows. As the spatial resolution between the radio sources in the pre-observation becomes shorter, the significantly more radio sources in the pre-observation phase are required. It is difficult to use all the constructed relationships for positioning because of huge computational complexity for selecting the most suitable location fingerprint vector from the constructed relationships and the necessity of huge data base. In addition, the location fingerprint vector is not so particular that the two radio sources with the quite small distance cannot be distinguished. In radio fingerprint positioning, the spatial resolution between the radio sources

in the pre-observation phase is limited and thus the position gap between the radio source in the pre-observation phase and that in the position-estimation phase is not completely avoidable.

The position fingerprint method requires packet transmission to send the RSSI and the transmitting station ID of all sensors. A method using polling [41] and a method using autonomous access [11] were proposed to gather information from all sensors in the packet access. In either method, each sensor requires an independent access timing to avoid packet collisions. Therefore, the time overhead for access control and the allocation of independent time resources to each sensor leads to an extremely long data-gathering time.

IV. PROPOSED METHOD: LOCATION FINGERPRINTING BY PhyC-SN

PhyC-SN is used when gathering sensor information from each sensor during location fingerprinting.

In the pre-observation phase, the RSSIs measured by the sensors were reported to the CS by PhyC-SN. The CS detects the number of notified sensors for each quantized RSSI level based on the frequency spectrum of the received signal. Next, the position fingerprint vector was generated by arranging the detected RSSI levels in descending order. Let $\tilde{p}_d^l$ be the dth magnitude RSSI at the lth source. The location fingerprint vector by the PhyC-SN notification at the lth source is as follows:

$$\tilde{\boldsymbol{p}}^l = [\tilde{p}_1^l, \tilde{p}_2^l, \ldots, \tilde{p}_{N_D}^l]. \tag{4}$$

The location fingerprint vectors were obtained from PhyC-SN notifications at various radio sources.

In the position-estimation phase, the CS sends a control signal to all sensors. Each sensor that receives the control signal notifies the measured RSSI by PhyC-SN. The CS obtains the position fingerprint vector by the PhyC-SN notification using the same procedure as the pre-observation phase, as shown in the following equation:

$$\tilde{\boldsymbol{p}}^* = [\tilde{p}_1^*, \tilde{p}_2^*, \ldots, \tilde{p}_{N_D}^*]. \tag{5}$$

Consequently, using the positional fingerprint vector from the PhyC-SN notification, the nearest radio source of the pre-observation phase is identified using the minimum squared Euclidean distance criterion. The following formula holds:

$$l^\star = \arg\min_{\forall l} (\tilde{\boldsymbol{p}}^* - \tilde{\boldsymbol{p}}^l)(\tilde{\boldsymbol{p}}^* - \tilde{\boldsymbol{p}}^l)^T. \tag{6}$$

The position of the radio source in the pre-observation phase at $l^\star$ was specified as the position of the radio source to be estimated.

PhyC-SN does not specify the sensor ID that measures the RSSI. If an error occurs when estimating the number of sensors at each RSSI level, then the size of the location fingerprint vector may be smaller or larger than the total number of sensors. If there were fewer gathered RSSI levels than the total number of sensors, we added the data of the lowest RSSI level and made the size of the location fingerprint vector equal to the total number of sensors. Otherwise, we delete the data from the small RSSI levels to make the size of the location fingerprint vector equal to the total number of sensors. To rearrange the RSSI in descending order when generating the position fingerprint vector, the process of adding or deleting the elements of the RSSI maintains the order of the position fingerprint vector. Therefore, adding or deleting data to the tail of the position fingerprint vector prevents a significant change from occurring with respect to the tendency of the position fingerprint vector.

A. ACCESS PROTOCOL FOR IMPROVING POSITION ACCURACY

To count the number of sensors selecting the subcarrier from the received signal in PhyC-SN, the fact that the magnitude of the power of the detected subcarrier is proportional to the number of sensors is used. In other words, multiple thresholds are prepared in the direction of the magnitude of the RSSI power, and the detected power is compared to identify the number of corresponding sensors. However, if the power fluctuates because of multipath fading or propagation loss, the identification accuracy is significantly degraded. Deterioration in the identification accuracy distorts the positional fingerprint vector, and a source far from the actual source is erroneously recognized as the nearest neighbor, resulting in a positioning error.

To improve the positioning accuracy, the multistage threshold for each subcarrier is limited to one stage. That is, for each subcarrier, we identify whether one or more sensors transmit or no sensor does; the identification is referred to as ''on-off identification''. Using receive diversity with multiple receiving antennas [42], the received signal attenuation can be stable. Therefore, when more than one sensor is transmitted, reliable detection is possible at the receiving station, and recognition errors of the sensor information owing to fluctuations in the received signal power can be avoided. However, the ''on-off identification'' cannot identify the number of sensors if more than one sensor selects the same subcarrier. Consequently, the recognition information is lost and the positioning accuracy deteriorates.

Figure 3(a) shows a heat map of the RSSI strength of each sensor detecting the emitted signal from the radio source. Figures 3(b) and (c) are the images of the RSSIs gathered by PhyC-SN with the determination of the number of sensors and with ''on-off identification,'' respectively. No identification errors occurred during this evaluation. The horizontal axis of the image indicates equally spaced subcarrier bands and each divided subcarrier corresponds to a unique quantized RSSI. The colors in Figure 3(b) indicate the number of sensors transmitted on the same subcarrier. However, black and white in Figure 3 (c) show the case where one or more sensors are transmitted and the case where none of the sensors are transmitted, respectively. The three figures have sources at the same locations. As shown in the figure, three-dimensional

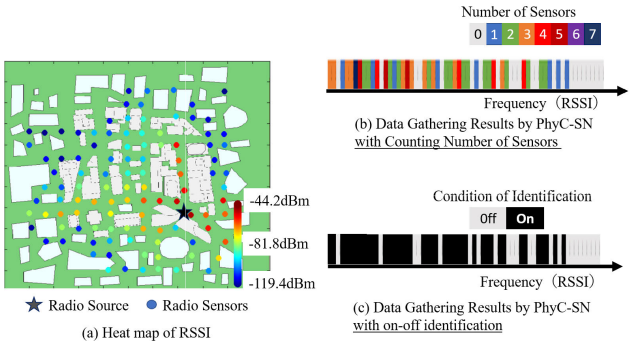

FIGURE 3. Heat map of radio monitoring and results of data gathering by PhyC-SN.

data, including sensor planar deployment and the RSSI intensity, are gathered by PhyC-SN and projected onto the frequency axis. The number of sensors that detect each RSSI can be determined in Figure 3(b), similar to the one-dimensional histogram. Figure 3 (c) loses information on the number of sensors, hence the actual 3D heat map features are limited compared to figure3(b), but not completely lost.

B. COMBINED USE OF PhyC-SN TIME-DIVISION TRANSMISSION AND GROUP FORMATION CONSIDERING AREA

In the ''on-off identification'', the RSSI, which is the reported sensor information, is lost when one or more sensors select the same subcarrier. We propose time-division multiple access for each group. In the proposed time-division multiple access, the simultaneous accessing groups of sensors are set, different access timings are assigned to each group, and then all the sensors within the group simultaneously access the CS. If the total number of access timings is $N_T \in 1, 2, \ldots$, the number of sensors notified in the same time slot is at most $\lceil N_D/N_T \rceil$, where N_D is the total number of sensors and $\lceil \cdot \rceil$ is the ceiling function. Consequently, the number of sensors notified at the same time can be reduced, and the possibility of selecting the same subcarrier can be reduced.

The RSSI measured by each sensor was spatially correlated. If the source emits radio waves with an omnidirectional antenna, the radio waves spread on the spherical surface. Sensors that are uniformly distributed on a two-dimensional plane detect the same RSSI if they are located at the same distance from the radio source, and there is no reflecting object in the free space. The similarity of the RSSI exists in real-world environments with reflective objects depending on the distance of each sensor from the source. Because of such RSSI similarities between sensors, multiple sensors may select the same subcarrier for data gathering by PhyC-SN. To suppress this similarity, when forming simultaneous access groups of sensors, the positional relationship of the sensors within the observation area was considered.

We assume there are $N_{D,g}$ sensors in the gth group ($g \in 1, 2, \ldots, N_G$), where N_G is the number of groups. The

Packet Access				
Sensor ID	1	2	3	4
Location fingerprint vector in #1 radio source (dBm)	-60	-50	-45	-65
Location fingerprint vector in #2 radio source (dBm)	-45	-65	-60	-50

PhyC-SN without Group Dvision				
Sensor ID	N/A	N/A	N/A	N/A
Location fingerprint vector in #1 radio source (dBm)	-45	-50	-60	-65
Location fingerprint vector in #2 radio source (dBm)	-45	-50	-60	-65

PhyC-SN with Group Division				
Group of Sensor	Group#1	Group#1	Group#2	Group#2
Location fingerprint vector in #1 radio source (dBm)	-50	-60	-45	-65
Location fingerprint vector in #2 radio source (dBm)	-45	-65	-50	-60

FIGURE 4. Example of location fingerprint vector in each data gathering scheme.

position fingerprint vector of each group was generated by arranging the detected RSSI levels in descending order. Note that the position fingerprint vector was generated in group by group. Let $\tilde{p}^l_{d,g}$ be the dth magnitude RSSI of the gth group at the lth source in the pre-observation phase. The location fingerprint vector of the lth radio source in the gth group is given by

$$\tilde{\boldsymbol{p}}^l_g = [\tilde{p}^l_{1,g}, \tilde{p}^l_{2,g}, \ldots, \tilde{p}^l_{N_{D,g},g}]. \tag{7}$$

In the position-estimation phase, the location fingerprint vector of the radio source in the gth group is

$$\tilde{\boldsymbol{p}}^*_g = [\tilde{p}^*_{1,g}, \tilde{p}^*_{2,g}, \ldots, \tilde{p}^*_{N_{D,g},g}]. \tag{8}$$

The nearest radio source of the pre-observation phase is identified using the minimum squared Euclidean distance criterion. The following formula holds:

$$l^\star = \arg\min_{\forall l} \sum_{g=1}^{N_G} (\tilde{\boldsymbol{p}}^*_g - \tilde{\boldsymbol{p}}^l_g)(\tilde{\boldsymbol{p}}^*_g - \tilde{\boldsymbol{p}}^l_g)^T. \tag{9}$$

For clarifying the difference of the location fingerprint vectors among the data gathering schemes, Figure 4 shows the example of the location fingerprint vectors in the packet access scheme, the PhyC-SN without the group division, and the PhyC-SN with the group division. We assume the two radio sources in the pre-observation phase and the radio source is different position to the other one. The constructed location fingerprint vector should be different for distinguishing the position of each radio source. In the PhyC-SN without group division, the two location fingerprint vectors constructed by the descending ordering of RSSIs are the same, each other. This is because the sensor Id of the informed RSSI is lost and then the particularity of the location fingerprint vector is lost. If we use the group division, we calculate

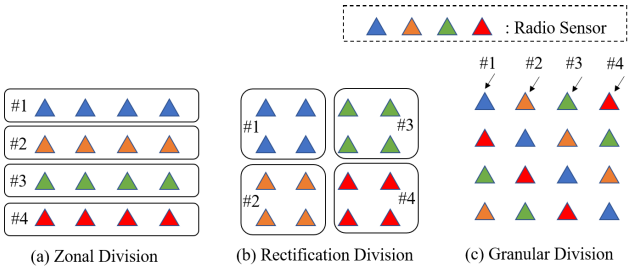

FIGURE 5. Group division format.

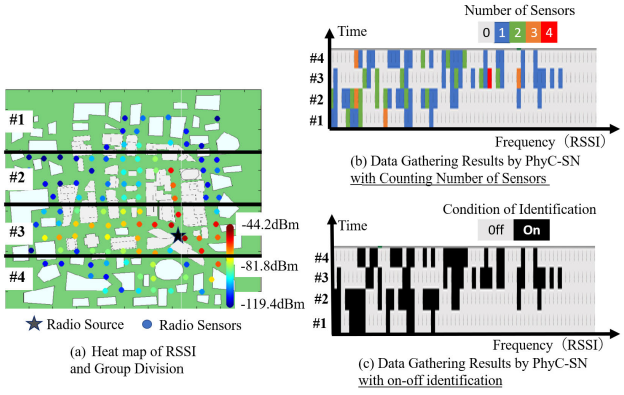

FIGURE 6. Heat map of radio monitoring and results of data gathering by PhyC-SN with zonal group division.

the location fingerprint vector constructed by the descending order in group by group. Since the location fingerprint vectors are different each other, these have particularity that these can be distinguished. Therefore, the radio sources in the pre-measurement phase can be distinguished with higher accuracy.

Three types of simultaneous access group formations were examined. Fig. 5 shows three types of groups. The first type is the zonal group. The observation area was divided horizontally or vertically to form areas, and each area was considered as one group. The second type is the square group. When the observation area was divided into squares, the areas were formed to form squares whose sides were as equal as possible. The third type is the granular group. Paying attention to the fact that the sensors are arranged in a row, different sensor group numbers are assigned from the top starting from 1, and when all the sensor group numbers have been assigned, they are assigned again from 1. Consequently, the sensors that belong to the same group are scattered, and the entire group has a shape that spreads uniformly over the observation area. The effects of time-division transmission and group formation are shown using a data-gathering example. Figure 6(a) shows a heat map of the RSSI observation results of each sensor at the source and the relationship between the monitoring area and zonal group division. Four groups were formed using the zonal group. The sensors in each group accessed the CS simultaneously, but those in the different

FIGURE 7. Sensor locations in computer simulation.

groups accessed the CS at different times. In Figure 6(b), the color of the PhyC-SN data-gathering result indicates the number of sensors accessed simultaneously, whereas in Figure 6(c), the monochrome indicates the case where one or more sensors are accessed and the case where none of the sensors is accessed. It can be observed that the spatial features of the sensors spread over two dimensions can be captured simultaneously by the access group and time-division transmission. Compared with Figure 3(b), the subcarriers selected by two or more sensors are reduced in Figure 6(b). By combining the time-division transmission and group formation in this manner, it is possible to suppress duplication in which sensors transmit the same subcarrier. Moreover, Figure 6(c) reflects more spatial features on the time and frequency axes than Figure 3(c); therefore, the source identification accuracy is expected to improve.

V. SIMULATION RESULTS

Radio wave propagation was simulated using a ray tracing simulation. In the simulation environment, 136 sensors (Fig. 7) were placed at regular intervals in an urban space of 800 m $\times$ 800 m. The sensors were arranged at intervals of 50 m.

Figure 8 shows the position of the source during the pre-observation phase of the position fingerprinting method. Thirty-seven sources were placed and the position of each source was determined. The positions of the sources in the pre-observation phase were set at approximately equal intervals, with an interval of approximately 100 m.

The generation source to be estimated in the position estimation phase is set as follows. As shown in Figure 8, the source of the pre-observation phase and its adjacent source were paired, and the two locations were divided into 20 m intervals. Consequently, the target radio sources in the position estimation phase were set in the divided position. The divided positions were constructed from the five selected source pairs. In these settings, the positioning target was

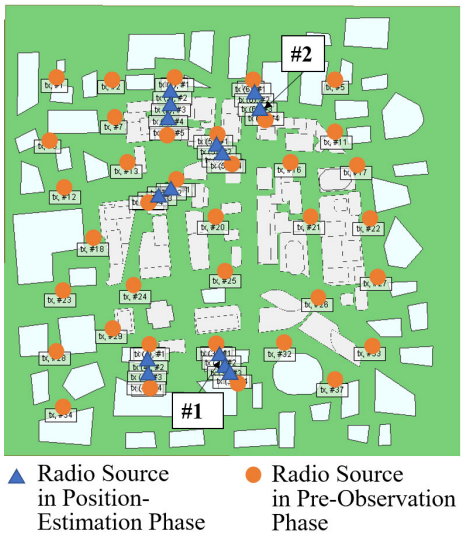

FIGURE 8. Position of radio sources.

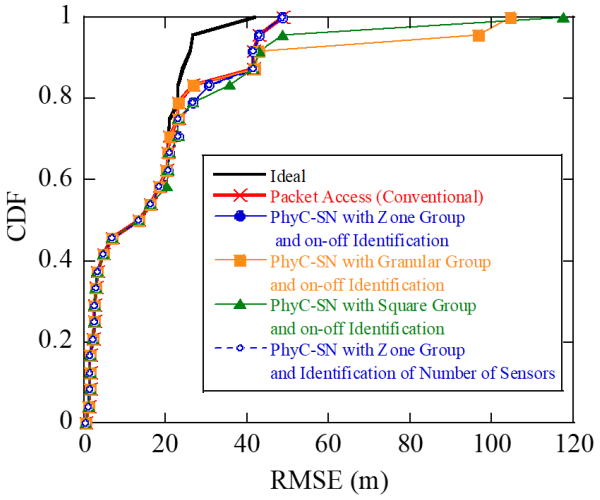

FIGURE 9. CDF of RMSE in various data gathering schemes.

TABLE 2. Configuration of LoRa (radio source).

Center frequency	920.6[MHz]
Bandwidth	0.125[MHz]
Transmit power	10[dBm]
Number of reflections	6
Diffraction number	1
Number of passes	0

changed at intervals narrower than the arrangement intervals of the sources in the pre-observation phase. It is difficult for fingerprinting positioning, and thus, we evaluate the position accuracy of each positioning scheme in the worst cases.

Table 2 lists the parameters of radio wave propagation at the source. In this evaluation, the source is a parameter conforming to the LoRa standard of a low-power wide area (LPWA).

We assume that the radio sensor detects the lowest and highest RSSI at −120dBm and −35 dBm, respectively. The quantization interval when transmitting the RSSI in PhyC-SN is the value obtained by dividing the interval between the lowest and highest RSSI by the total number of subcarriers minus one. It is assumed that transmission errors do not occur during wireless transmissions. When calculating the squared Euclidean distance between the position fingerprint vector of the pre-observation phase and that of the position estimation phase, the RSSI is calculated using the dBm domain values.

A. SIMULATION RESULTS

Fig. 9 shows the cumulative distribution function (CDF) performance for the root mean square error (RMSE), where the RMSE is defined as the value of the square root of error between the actual position of the radio source and estimated position and it is defined as follows.

$$\mathrm{RMSE} = \sqrt{(\boldsymbol{r_t} - \boldsymbol{r_e})^2} \tag{10}$$

where $\boldsymbol{r_t}$ and $\boldsymbol{r_e}$ are the true position vector and the estimated one of the radio source, respectively. The position vector is composed of the two coordinates of x-axis and y-axis. In addition, Table 3 shows the measurement results of the two radio sources with unknown position, where figure 8 shows the positions of the two resources. The conventional method and PhyC-SN are respectively the case of data gathering by packet access and the proposed PhyC-SN. In PhyC-SN, the number of subcarriers was 128, the time-division transmission and group formation were used, and the number of time divisions was eight. Simultaneous access groups are formed in three ways: zone, square, and granular. In the packet access scheme, assuming data gathering by time-division multiple access, each sensor is assigned a particular time slot to access the CS. Therefore, the time required for data gathering was 136 time slots, which is equal to the total number of sensors. However, PhyC-SN requires eight time slots, which is the number of area divisions, because the sensors within the group access the CS in the same time slot. Therefore, the time required for data gathering is reduced to approximately 1/17 or less than that of the packet access scheme, and thus the PhyC-SN realizes high speed. In PhyC-SN, the ''on-off identification'' is applied to three types of group formations: zone, square, and granular groups. For comparison, the results of ''identification of the number of sensors'' are shown assuming that the number of sensors transmitting each subcarrier can be identified without any error only for the zone group of PhyC-SN. Additionally, the number of subcarriers used in PhyC-SN is 128.

The ''Ideal'' of figure 9 is the case where the source of the pre-observation process, which is the nearest neighbor to the source to be estimated, is estimated without error. It achieves the best estimation accuracy in the fingerprinting method, and thus corresponds to the upper bound of the estimation accuracy.

TABLE 3. Numerical example of estimation accuracy.

Unknown Target Location	Actual Coordinates	Ideal	Packet Access (Conventional)	PhyC-SN with Zonge Group and on-off Identification (Proposed)	PhyC-SN with Granular Group and on-off Identification (Proposed)	PhyC-SN with Square Group and on-off Identification (Proposed)	PhyC-SN with Zone Group and Identification of Number of Sensors (Proposed)
Coordication of #1 Radio Source	(100.83,-121.01)	(90.07,-103.47)	(123.47,-155.67)	(123.47,-155.67)	(204.31,-106.15)	(123.47,-155.67)	(123.47,-155.67)
RMSE of #1 Radio Source (m)		20.58	41.40	41.40	104.54	41.40	41.40
Coordication of #2 Radio Source	(164.04,328.53)	(182.64,326.58)	(152.84,384.67)	(152.84,384.67)	(87.43,285.56)	(109.03,240.73)	(152.84,384.67)
RMSE of #2 Radio Source (m)		25.90	41.61	41.61	96.72	117.54	41.61

Figure 9 shows that "Packet Access," "PhyC-SN with Zone Group and on-off identification," and "PhyC-SN with Zone Group and Sensor Number Identification" achieve the same position accuracy at the CDF = 1.0, where the CDF = 1.0 is the worst accuracy of the position estimation. These achieve the 5% degradation of the position accuracy compared to the "Ideal". Notably, "Packet Access" requires considerably larger time slots than "PhyC-SN with Zone and on-off identification". Therefore, "PhyC-SN with Zone Group and on-off Identification" achieves a good position accuracy with a much smaller data-gathering time. Furthermore, it is possible to omit the identification of the number of sensors, and thus, it is possible to secure a high resistance to the received power fluctuations caused by radio propagation.

"PhyC-SN with Square Group and on-off identification" and "PhyC-SN with Granular Group and on-off identification" achieve the worst position accuracy than "PhyC-SN with Zone Group and on-off identification". Their RMSEs at CDF = 1.0 are significantly degraded. The reasons for this are as follows: The zone and square groups are constructed by dividing the observation area into regions so that the characteristics of the region can be detected from the RSSIs informed in the particular access timing. However, in the granular group, sensors that report at the same time are uniformly distributed in the observation area; therefore, there is little regional difference in space over time. Furthermore, the spatial feature trends of RSSI become rough, resulting in a deterioration in the accuracy of identifying the spatial feature trends. Consequently, the position estimation accuracy of the radio source deteriorated. In the square and zone groups, the RSSI tendency of the local site is separately recognized owing to the time division of data gathering. The sensors within each granular group were widely distributed over the entire monitoring area. The RSSI tendency informed by the sensors within each sensor is similar, and its spatial resolution is worse than that of the zone and square groups because the distance interval among the sensors in the granular group is larger than that in the zone and square groups. Consequently, the position accuracy of the former is worse than that of the latter.

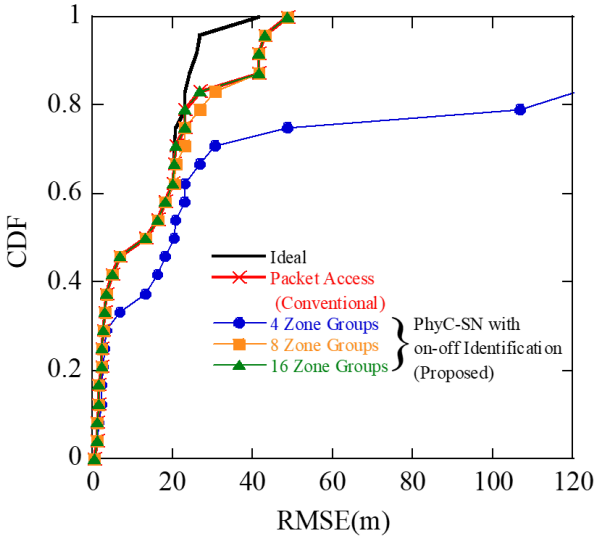

FIGURE 10. CDF of RMSE in various group numbers.

The mutual distances between the sensors in the square group were smaller than those in the zone group. Therefore, some sensors in the former detect a more similar RSSI than those in the latter. In PhyC-SN, the selection probabilities of the common subcarriers among sensors become larger, and thus, more informed RSSIs are deleted by the "on-off identification". Therefore, the position accuracy of the square group is degraded.

B. COMPARING NUMBER OF GROUP DIVISIONS

Figure 10 shows CDF characteristics in the RMSE for various numbers of groups. The zone group included and the number of subcarriers is 128. In the PhyC-SN, the "on-off identification" is used. For comparison, the positioning accuracies of "Ideal" and "Packet Access" are shown. As shown in the figure, increasing the number of area divisions improves the position accuracy. An increase in the number of area divisions caused an increase in the number of time divisions for data gathering, resulting in a longer time required for positioning recognition. The RMSE is significantly degraded when the

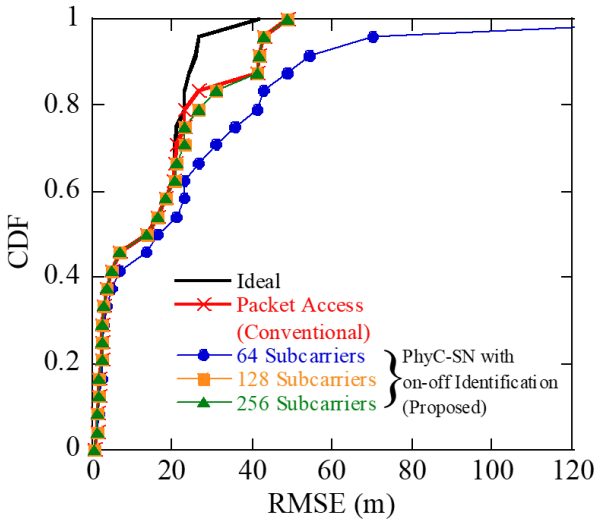

FIGURE 11. CDF of RMSE in various subcarrier numbers.

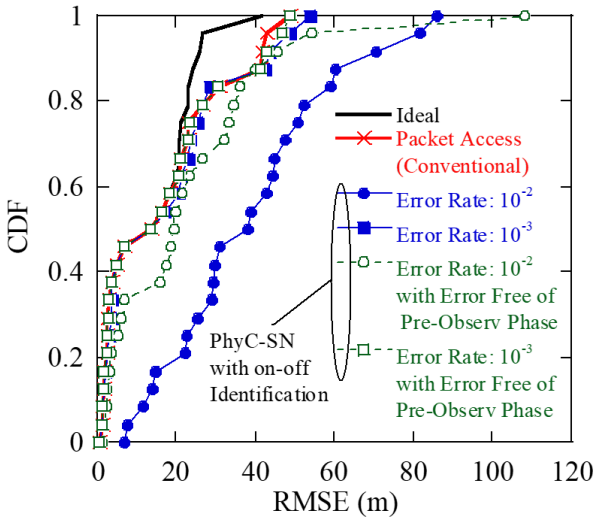

FIGURE 12. CDF of RMSE in gathering failures.

number of divisions is 4, whereas there is no difference in the RMSE at CDF=1.0 between the number of divisions of 8 and 16. An increase in the number of divisions results in a trade-off relationship between the time required for data gathering and positioning accuracy, and this relationship varies depending on the environment. In this evaluation environment, 8 is considered appropriate for the number of group divisions to achieve high-precision positioning accuracy in a short period of time.

C. COMPARISON OF NUMBER OF SUBCARRIERS

Figure 11 shows the CDF of RMSE for various subcarriers of PhyC-SN. For comparison, the "Ideal" and "Packet Access" results are also shown. The number of subcarriers was 64, 128, and 256 in PhyC-SN, respectively. Eight zone groups were used in this study. Additionally, the "on-off identification" is used. The figure shows that the RMSE was improved by increasing the number of subcarriers. As the number of subcarriers increases, the quantization interval of the RSSI becomes narrower, making it possible to identify a finer RSSI. Consequently, the possibility of multiple sensors selecting the same subcarrier is reduced, thus, the phenomenon of losing information on the number of sensors owing to "on-off identification" can be suppressed. An increase in the number of subcarriers results in an increase in the occupied bandwidth; therefore, in this evaluation environment, a total of 128 subcarriers are appropriate to achieve both excellent positioning accuracy and a small, occupied bandwidth.

D. EFFECT OF ERROR IN DATA GATHERING

Previous evaluations assumed that wireless access for data gathering is error-free. Next, we consider the effects of error on the wireless access of PhyC-SN with the "on-off identification". Fig. 12 shows the CDF in the RMSE. PhyC-SN uses 8 zone groups and 128 subcarriers. As a model of the identification error, we assumed the following two errors in the "on-off identification". In the first error identification, it is true that one or more sensors transmit the continuous wave of the subcarrier but it is recognized that no sensor transmits it. In the second error identification, it is true that no sensor transmits any wave of the subcarrier but one or more sensors do. Their error occurrences were modeled as random, and two occurrence probabilities, 10^{-2} and 10^{-3}, were assumed. Additionally, it is possible to suppress the occurrence of errors by increasing the received power and acquiring a time diversity effect. The time loss required to obtain the time diversity effect can be accepted in the pre-observation phase. Therefore, we also evaluated the case where error occurrence cannot and can be avoided in the estimation and pre-observation phases, respectively. For comparison, the results of the "Ideal" and "Packet Access" are also shown, where error free is assumed in "Packet Access".

From the figure, when the error probability is 10^{-3}, the result is equivalent to no misjudgment regardless of the presence or absence of errors during the pre-observation phase. However, when the error probability degrades to 10^{-2}, the RMSEs with and without the error of the pre-observation phase are 20 m and 8 m larger than those without any error, respectively. Although significant degradation at $CDF = 1.0$ is confirmed, in the other cases, the PhyC-SN without the error of the pre-observation phase usually achieves a good position estimation accuracy. It is important to avoid the error for the pre-observation phase, and the error probability of recognizing the signal in each subcarrier should be smaller than 10^{-2}.

VI. EXPERIMENTAL EVALUATION OF RADIO SOURCE MONITORING

The experimental evaluation of radio source monitoring was conducted using an actual wireless device. We assume that

FIGURE 13. Radio source in 920 MHz band LoRa gateway.

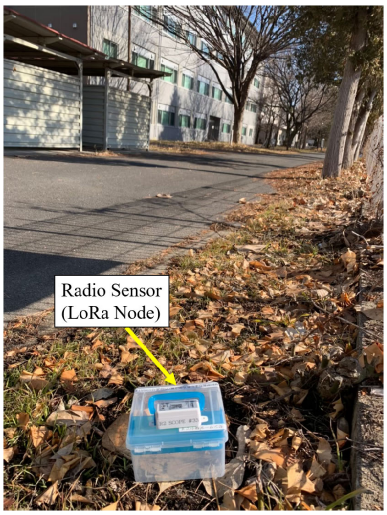

FIGURE 14. Radio sensor in 920 MHz band LoRa node.

the CS and radio sensor of the 920 MHz band LoRa are the radio source and radio sensor, respectively, where the former and latter are the Dragino LoRaWAN gateway (LPS8-JP, figure(13)) and a Dragino (LHT65), figure(14), respectively. To measure the RSSI, the radio sensor transmits the signal to the CS, which then measures the RSSI from the received signal. Based on the symmetry of radio propagation, we can assume that the RSSI from the radio sensor to the CS is the same as that from the CS to the radio sensor. Therefore, the RSSI measured by the CS was considered to be that measured by the radio sensor. Additionally, in this experimental evaluation, packet data gathering and PhyC-SN of the RSSI measurement results of each sensor were performed by simulation. It is assumed that packet and identification errors do not occur during data gathering. It should be noted that the 920 MHz band LoRa in this experiment was used for positioning the radio source and was not used for data gathering.

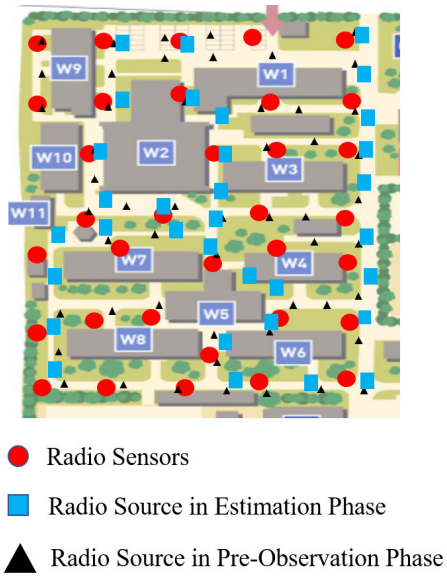

FIGURE 15. Positions of radio sensors and sources.

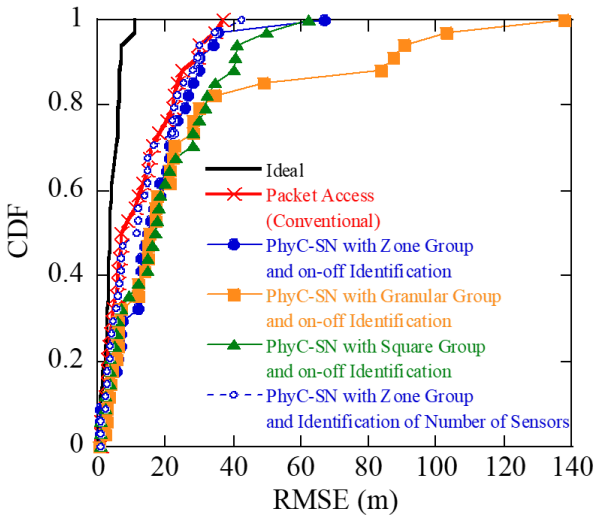

FIGURE 16. CDF of RMSE in experimental results.

Fig. 15 shows the sensor arrangement (red circle), the position of the radio source in the pre-observation phase (black triangle), and the position of the radio source in the estimation phase (blue square). There were 34 sensors, 74 radio source positions for the pre-observation phase, and 35 radio source positions for the estimation phase. The observation area is $190 \times 110[\mathrm{m}^2]$. In the proposed method, PhyC-SN, the number of groups is four, and the number of subcarriers is 128.

Fig. 16 shows the CDF of the RMSE. Figure 16 shows the results for "Ideal" and "Packet Access". In the proposed method of PhyC-SN, there are three types of groups: zone, square, and granular groups, and the "on-off identification. For comparison, we show the results using PhyC-SN's "identification of the number of sensors" and the four zone groups.

The RMSE of ''Ideal'' in this figure is smaller than that of figure 9. This reason is as follows. The minimum distances between the two radio sources in the pre-observation phase are about 100 m in figure 9 and about 10 m in figure 16. As the minimum distance between the two radio sources becomes smaller, the position gap between the radio source in the pre-observation phase and that in the position-estimation phase is smaller.

From this figure, compared to ''Ideal'', ''Packet Access'' and ''PhyC-SN with Zone Group and Identification of Number of Sensors'' are degraded by approximately 30 m at CDF = 1.0. From Figure 16, it is considered that the identification accuracy deteriorated because tall buildings are regularly arranged, and the position-specific RSSI distribution of the radio sensors has a highly partial correlation. ''Packet Access'' and ''PhyC-SN with Zone Group and Identification of Number of Sensors'' achieve almost the same position accuracy. The time required to aggregate the number of sensors was 34 time slots for the former conventional method and four time slots for the latter proposed method, significantly reducing the time required for data gathering. Moreover, ''PhyC-SN with zone group and on-off identification'' deteriorates by approximately 8 m on average compared to ''Packet Access'' and significant deterioration occurred only at CDF = 1.0. The performance degradation is that the loss of information on the number of sensors distorts the measured RSSI distribution, which causes the deterioration in accuracy. However, it has a high resistance to power fluctuations during data gathering through wireless communication, which is realistic. Additionally, ''PhyC-SN with zone group'' achieved superior positioning accuracy compared to ''PhyC-SN with square group'' and ''PhyC-SN with Granular Group'' except for CDF = 1.0 points, indicating the superiority of the zone group. From this, it is confirmed that the proposed method achieves excellent positioning accuracy even in an actual radio-monitoring environment.

VII. CONCLUSION

This study proposed a fingerprint position estimation method using sensor information data gathering by physical wireless parameter conversion sensor networks (PhyC-SN), which does not require the complicated access control and gather sensing data from many sensors. In the proposed method, to estimate the position of the radio source, when transmitting the RSSI measured by each sensor with PhyC-SN, the ''on-off identification'' method using one threshold judgment to suppress the influence of power fluctuation was adopted. To suppress the distortion of the aggregation results due to ''on-off identification,'' we proposed the construction of a sensor group for assigning a particular accessing time slot to each group based on time-division multiple access. We clarified the suitable shape of the group for avoiding duplication of the sensing data and detecting the RSSI distribution tendency. Through computer simulations and experimental evaluation, the time required for aggregation was significantly reduced compared with aggregation by conventional packet communication; high-precision position estimation accuracy was achieved.

In the computer simulation, we do not assume any channel model. The evaluation of positioning accuracy under the wireless communication through the practical channel model is an important future work. The system limitations are decided by the frequency bandwidth for subcarrier selection. As the usable frequency bandwidth is larger, the number of subcarriers becomes larger. Thus, the sensing data loss by the on-off identification is more effectively avoided. For securing the frequency bandwidth, the frequency spectrum sharing between the other wireless system and the PhyC-SN is necessary. However, the spectrum appearance caused by the wireless access from the other system causes the misunderstanding of the continuous signal sent by the sensor. Therefore, distinguishing between the continuous signal sent by the sensor and the other signal should be required and thus its construction is important future work.

REFERENCES

[1] X. Guo, N. Ansari, L. Li, and L. Duan, ''A hybrid positioning system for location-based services: Design and implementation,'' *IEEE Commun. Mag.*, vol. 58, no. 5, pp. 90–96, May 2020.

[2] P. G. Avila, S. N. Karels, T. J. Macdonald, G. A. Matchett, I. P. Roberts, and V. Gloster, ''An overview of a global positioning system mission planner implemented on a personal computer,'' *IEEE Aerosp. Electron. Syst. Mag.*, vol. 5, no. 1, pp. 10–18, Jan. 1990.

[3] Z. Wu and Y. Yin, ''Influence of heat source location on heat dissipation performance of an underwater scientific instrument interface module,'' in *Proc. 4th World Conf. Mech. Eng. Intell. Manuf. (WCMEIM)*, Nov. 2021, pp. 453–457.

[4] R. Fujita, H. Yoshida, M. Hori, and M. L. L. Wijerathne, ''Evacuation simulation regarding building damage caused by earthquake,'' *J. Jpn. Soc. Civil Eng., Ser. A2 Appl. Mech. (AM)*, vol. 71, no. 2, pp. I_643–I_654, 2015.

[5] Ministry of Internal A Airs and Communications Japan. *DEURAS Direction Finder (DEURAS-D)*. Accessed: Nov. 28, 2022. [Online]. Available: http://www.tele.soumu.go.jp/e/adm/monitoring/moni/type/deurasys/deurasd.htm

[6] H. Matsuno, Y. Kunisawa, and T. Hayashi, ''Direction and location estimation algorithm with power gravity point for spectrum sharing,'' in *Proc. Int. Symp. Antennas Propag. (ISAP)*, Jan. 2021, pp. 679–680.

[7] M. Miyashita, ''Influence of diffraction for wireless sensor node positioning using audible tone,'' *IEICE Tech. Rep.*, vol. 116, no. 145, pp. 57–62, Jul. 2016.

[8] T. Tsujino and T. Fujii, ''Precise position estimation using position fingerprinting using time-series received data,'' *IEICE Tech. Rep.*, vol. 120, no. 74, pp. 169–174, Jun. 2020.

[9] R. Kovalchukov, D. Moltchanov, J. Pirskanen, J. Sae, J. Numminen, Y. Koucheryavy, and M. Valkama, ''DECT-2020 new radio: The next step toward 5G massive machine-type communications,'' *IEEE Commun. Mag.*, vol. 60, no. 6, pp. 58–64, Jun. 2022.

[10] U. Raza, P. Kulkarni, and M. Sooriyabandara, ''Low power wide area networks: An overview,'' *IEEE Commun. Surveys Tuts.*, vol. 19, no. 2, pp. 855–873, 2nd Quart., 2017.

[11] T. Suehiro, T. Kobayashi, O. Takyu, and Y. Fuwa, ''Data gathering scheme for event detection and recognition in low power wide area networks,'' *IEICE Trans. Commun.*, vol. E106-B, no. 8, Aug. 2023.

[12] H.-S. Nguyen, T.-S. Nguyen, P. T. Tin, and M. Voznak, ''Outage performance of time switching energy harvesting wireless sensor networks deploying NOMA,'' in *Proc. IEEE 20th Int. Conf. e-Health Netw., Appl. Services (Healthcom)*, Sep. 2018, pp. 1–4.

[13] Q. Ni, M. Yang, S. A. Odhano, M. Tang, P. Zanchetta, X. Liu, and D. Xu, ''A new position and speed estimation scheme for position control of PMSM drives using low-resolution position sensors,'' *IEEE Trans. Ind. Appl.*, vol. 55, no. 4, pp. 3747–3758, Jul. 2019.

[14] A. Sahoo, N. El Ouni, and V. Shenoy, "A study of timing constraints and SAS overload of SAS-CBSD protocol in the CBRS band," in *Proc. IEEE Globecom Workshops (GC Wkshps)*, Dec. 2019, pp. 1–6.
[15] O. Takyu, K. Shirai, T. Fujii, and M. Ohta, "Adaptive channel assignment with predictions of sensor results and channel occupancy ratio in PhyC-SN," *IEEE Access*, vol. 7, pp. 44645–44658, 2019.
[16] S. M. Kay, *Fundamentals Stat. Signal Processing: Detection Theory*. Upper Saddle River, NJ, USA: Prentice-Hall, 1998.
[17] M. Oda and O. Takyu, "Position estimation with radio sensor in physical wireless parameter conversion sensor networks," in *Proc. IEICE*, Dec. 2021, p. P4.
[18] M. Oda and O. Takyu, "Area model for position estimation with radio sensor in physical wireless parameter conversion sensor networks," in *Proc. ICETC*, Dec. 2021, p. P4.
[19] Y. Xie, "An optimized three-dimensional positioning algorithm for RSSI-based wireless sensor network," in *Proc. 3rd Int. Conf. Intell. Control, Meas. Signal Process. Intell. Oil Field (ICMSP)*, Jul. 2021, pp. 30–33.
[20] W. Chen, "Research on improving positioning accuracy of sensor networks," in *Proc. IEEE 20th Int. Conf. Commun. Technol. (ICCT)*, Oct. 2020, pp. 841–845.
[21] T. H. Loh and H. Lin, "On the improvement of positioning accuracy in wireless sensor network using smart antennas," in *Proc. IEEE 8th Int. Conf. Commun. Netw. (ComNet)*, Oct. 2020, pp. 1–4.
[22] J. Huang, "Research on secure location algorithm for wireless sensor networks based on deep learning," in *Proc. 2nd Int. Seminar Artif. Intell., Netw. Inf. Technol. (AINIT)*, Oct. 2021, pp. 128–133.
[23] H. X. Jian and W. Hao, "WiFi indoor location optimization method based on position fingerprint algorithm," in *Proc. Int. Conf. Smart Grid Electr. Autom. (ICSGEA)*, May 2017, pp. 585–588.
[24] H.-W. Chan, A. I.-C. Lai, and R.-B. Wu, "Transfer learning of Wi-Fi FTM responder positioning with NLOS identification," in *Proc. IEEE Topical Conf. Wireless Sensors Sensor Netw. (WiSNeT)*, Jan. 2021, pp. 23–26.
[25] W. Ji, K. Zhao, Z. Zheng, C. Yu, and S. Huang, "Multivariable fingerprints with random forest variable selection for indoor positioning system," *IEEE Sensors J.*, vol. 22, no. 6, pp. 5398–5406, Mar. 2022.
[26] W. Wang, Q. Zhu, Z. Wang, X. Zhao, and Y. Yang, "Research on indoor positioning algorithm based on SAGA-BP neural network," *IEEE Sensors J.*, vol. 22, no. 4, pp. 3736–3744, Feb. 2022.
[27] C.-Y. Chen, A. I.-C. Lai, and R.-B. Wu, "Multi-detector deep neural network for high accuracy Wi-Fi fingerprint positioning," in *Proc. IEEE Topical Conf. Wireless Sensors Sensor Netw. (WiSNeT)*, Jan. 2021, pp. 37–39.
[28] K. Chen, C. Wang, Z. Yin, H. Jiang, and G. Tan, "Slide: Towards fast and accurate mobile fingerprinting for Wi-Fi indoor positioning systems," *IEEE Sensors J.*, vol. 18, no. 3, pp. 1213–1223, Feb. 2018.
[29] M. U. Ali, S. Hur, and Y. Park, "IoT enabled Wi-Fi indoor positioning system using raster maps," in *Proc. 18th Int. Conf. Inf. Process. Sensor Netw.*, Apr. 2019, pp. 327–328.
[30] G. Berkovich, D. Churikov, J. Georgy, and C. Goodall, "Coursa venue: Indoor navigation platform using fusion of inertial sensors with magnetic and radio fingerprinting," in *Proc. 22th Int. Conf. Inf. Fusion (FUSION)*, Jul. 2019, pp. 1–6.
[31] L.-F. Shi, Y. Wang, G.-X. Liu, S. Chen, Y.-L. Zhao, and Y.-F. Shi, "A fusion algorithm of indoor positioning based on PDR and RSS fingerprint," *IEEE Sensors J.*, vol. 18, no. 23, pp. 9691–9698, Dec. 2018.
[32] Y. Wu, R. Chen, W. Li, Y. Yu, H. Zhou, and K. Yan, "Indoor positioning based on walking-surveyed Wi-Fi fingerprint and corner reference trajectory-geomagnetic database," *IEEE Sensors J.*, vol. 21, no. 17, pp. 18964–18977, Sep. 2021.
[33] A. Yazici, S. B. Keser, and S. Gunal, "Integration of classification algorithms for indoor positioning system," in *Proc. Int. Conf. Comput. Sci. Eng. (UBMK)*, Oct. 2017, pp. 267–270.
[34] M. Sridharan, J. Bigham, C. Phillips, and E. Bodanese, "Collaborative location estimation for confined spaces using magnetic field and inverse beacon positioning," in *Proc. IEEE Sensors*, Oct. 2017, pp. 1–3.
[35] A. Belmonte-Hernandez, G. Hernandez-Penaloza, D. M. Gutierrez, and F. Alvarez, "Recurrent model for wireless indoor tracking and positioning recovering using generative networks," *IEEE Sensors J.*, vol. 20, no. 6, pp. 3356–3365, Mar. 2020.
[36] L. Cheng, Y. Li, M. Zhang, and C. Wang, "A fingerprint localization method based on weighted KNN algorithm," in *Proc. IEEE 18th Int. Conf. Commun. Technol. (ICCT)*, Oct. 2018, pp. 1271–1275, doi: 10.1109/ICCT.2018.8600210.
[37] B. Wang, X. Gan, X. Liu, B. Yu, R. Jia, L. Huang, and H. Jia, "A novel weighted KNN algorithm based on RSS similarity and position distance for Wi-Fi fingerprint positioning," *IEEE Access*, vol. 8, pp. 30591–30602, 2020.
[38] N. Mutoh and T. Shibata, "An indoor positioning system using a wearable wireless sensor and the support vector machine," in *Proc. IEEE Asia–Pacific Microw. Conf. (APMC)*, Dec. 2019, pp. 616–6182019.
[39] R. SambathKumar, S. Gowshameed, and S. Arunmozhi, "Arithmetical analysis of WSN based indoor positioning localization systems with Kalman filtering," in *Proc. Int. Conf. Syst., Comput., Autom. Netw. (ICSCAN)*, Jul. 2021, pp. 1–5.
[40] H. Hijazi, N. Kandil, N. Zaarour, and N. Hakem, "A new gradient descent positioning method in wireless sensor network based on received signal strength," in *Proc. IEEE Int. Symp. Antennas Propag. USNC-URSI Radio Sci. Meeting*, Jul. 2019, pp. 1809–1810.
[41] H. Lee and I. Park, "Performance of a receiver-initiated MAC protocol with aggregation for event-driven wireless sensor networks," in *Proc. Int. Conf. Inf. Netw. (ICOIN)*, Jan. 2018, pp. 853–856.
[42] R. Myoenzono, O. Takyu, K. Shirai, T. Fujii, M. Ohta, F. Sasamori, and S. Handa, "Data tracking and effect of frequency offset to simultaneous collecting method for wireless sensor networks," *Intnational J. Distrib. Sensor Netw.*, vol. 2015, pp. 1–10, Aug. 2015.

MASAFUMI ODA received the B.E. degree from the Department of Electrical and Electronic Engineering, Shinshu University, in 2021. His research interest includes wireless communication systems.

OSAMU TAKYU (Member, IEEE) received the B.E. degree in electrical engineering from the Tokyo University of Science, Chiba, Japan, in 2002, and the M.E. and Ph.D. degrees in open and environmental systems from Keio University, Yokohama, Japan, in 2003 and 2006, respectively. From 2003 to 2007, he was a Research Associate at the Department of Information and Computer Science, Keio University. From 2004 to 2005, he was a Visiting Scholar at the School of Electrical and Information Engineering, The University of Sydney. From 2007 to 2011, he was an Assistant Professor at the Department of Electrical Engineering, Tokyo University of Science. From 2011 to 2013, he was an Assistant Professor at the Department of Electrical and Electronic Engineering, Shinshu University, where he has been an Associate Professor, since 2013. His current research interests include wireless communication systems and distributed wireless communication technology. He was a recipient of the Young Researcher's Award of IEICE 2010 and the 2010 Active Research Award in radio communication systems from the IEICE Technical Committee on RCS.

MAI OHTA (Member, IEEE) received the B.E., M.E., and Ph.D. degrees in electrical engineering from The University of Electro-Communications, Tokyo, Japan, in 2008, 2010, and 2013, respectively. Since 2013, she has been an Assistant Professor at the Department of Electronics Engineering and Computer Science, Fukuoka University. Her research interests include cognitive radio, spectrum sensing, LPWAN, and sensor networks. She received the Young Researcher's Award from IEICE, in 2013.

TAKEO FUJII (Member, IEEE) was born in Tokyo, Japan, in 1974. He received the B.E., M.E., and Ph.D. degrees in electrical engineering from Keio University, Yokohama, Japan, in 1997, 1999, and 2002, respectively. From 2000 to 2002, he was a Research Associate at the Department of Information and Computer Science, Keio University. From 2002 to 2006, he was an Assistant Professor at the Department of Electrical and Electronic Engineering, Tokyo University of Agriculture and Technology. From 2006 to 2014, he was an Associate Professor at the Advanced Wireless Communication Research Center, The University of Electro-Communications. Currently, he is a Professor with the Advanced Wireless and Communication Research Center, The University of Electro-Communications. His current research interests include cognitive radio and ad-hoc wireless networks. He received the Best Paper Award in the IEEE VTC 1999-Fall; the 2001 Active Research Award in radio communication systems from IEICE Technical Committee of RCS; the 2001 Ericsson Young Scientist Award; the Young Researcher's Award from the IEICE in 2004; the Young Researcher Study Encouragement Award from IEICE Technical Committee of AN, in 2009; the Best Paper Award in IEEE CCNC 2013; and the IEICE Communication Society Best Paper Award, in 2016.

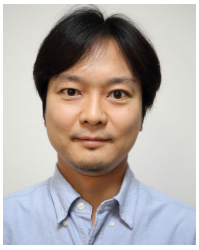

KOICHI ADACHI (Senior Member, IEEE) received the B.E., M.E., and Ph.D. degrees in engineering from Keio University, Japan, in 2005, 2007, and 2009, respectively.

From 2007 to 2010, he was a Research Fellow at the Japan Society for the Promotion of Science (JSPS). He was a Visiting Researcher at the City University of Hong Kong, in April 2009, and a Visiting Research Fellow at the University of Kent, from June 2009 to August 2009. From May 2010 to May 2016, he was with the Institute for Infocomm Research, A*STAR, Singapore. He is currently an Associate Professor with The University of Electro-Communications, Japan. His research interests include cooperative communication and energy-efficient communication technologies.

Dr. Adachi is a member of IEICE. He was awarded an Excellent Editor Award from IEEE ComSoc MMTC, in 2013. He is the coauthor of the WPMC 2020 Best Student Paper Award. He served as the General Co-Chair for the 10th and 11th IEEE Vehicular Technology Society Asia Pacific Wireless Communications Symposium (APWCS); the Track Co-Chair for the Transmission Technologies and Communication Theory of the 78th and 80th IEEE Vehicular Technology Conference, in 2013 and 2014, respectively; the Symposium Co-Chair for the Communication Theory Symposium of the IEEE GLOBECOM 2018 and the Wireless Communications Symposium of the IEEE GLOBECOM 2020; and the Tutorial Co-Chair for the IEEE ICC 2019. He has been an Associate Editor of *IET Transactions on Communications*, since 2015 and 2017; IEEE Wireless Communications Letters, since 2016; IEEE Transactions on Vehicular Technology, since 2016 and 2018; IEEE Transactions on Green Communications and Networking, since 2016; and IEEE Open Journal of Vehicular Technology, since 2019. He was recognized as an Exemplary Reviewer from the IEEE Wireless Communications Letters, in 2012, 2013, 2014, and 2015.